SUDDEN SOLVENT EVAPORATION IN BUBBLE ELECTROSPINNING FOR FABRICATION OF UNSMOOTH NANOFIBERS

by

Lei ZHAO[a,b], Peng LIU[a], and Ji-Huan HE[a*]

[a] National Engineering Laboratory for Modern Silk, College of Textile and Clothing Engineering, Soochow University, Suzhou, China
[b] College of Textile and Clothing, Yancheng Institute of Industry Technology, Yancheng, China

Original scientific paper
https://doi.org/10.2298/TSCI160725075Z

Solvent fraction in a multiple solvent system plays a great important for controlling fiber morphology in the bubble electrospinning. The sudden release of air pressure when a polymer bubble is broken and an extremely high velocity of jets are two main factors for solvent evaporation, which can be used for fabrication of unsmooth fibers.

Key words: *composite, nanofiber, bubble electrospinning, unsmooth structure, diameter, water contact angle*

Introduction

Nanoscale porous fibers have much more applications than smooth nanofibers. In this paper we will study a multiple solvent system in the bubble electrospinning for fabrication of PS/PVP composite nanofibers, PS (polystyrene) is an amorphous polymer and has good stability [1], and it can be easily dissolved in dimethyl formamide (DMF) [2], and PVP (polyvinylpyrrolidone) is a newly developed material which is a compound of PVC (polyvinylchloride) and PP (polypropylene) [3, 4], the former has excellent hydrophilic while the later has good flexibility [5].

Experimental

We prepared six samples for spun solution. The samples A and B were, respectively, 20 wt.% and 17.9 wt.% PS solutions with DMF solvent. The sample C was 27.27 wt.% polyvinilpyrrolidone (PVP) solution with C_2H_5OH as solvent; The sample D was prepared by dropping sample C into sample B gradually, till the resultant solution became agglomerated, see fig. 1(b). The sample E was 20 wt.% PS/PVP (mass mixing ratio of 7:3) with DMF as solvent. The sample F was prepared by dropping C_2H_5OH into sample E till the solution became agglomerated, fig. 1(c). The spinning process by the bubble electrospinning was illustrated in fig. 2, where the voltage was kept as 20 kV and the receipt distance was 13 cm.

Solvent evaporation

Sudden solvent evaporation occurs when air pressure decreases greatly and suddenly. During the bubble electrospinning or bubbfil spinning [3-8], an air-flow is input into the spun solution with a high pressure, and a polymer bubble is formed on the surface. When the bubble is broken, a sudden pressure drop is happened, and solvent evaporation occurs which

* Corresponding author, e-mail: hejihuan@suda.edu.cn

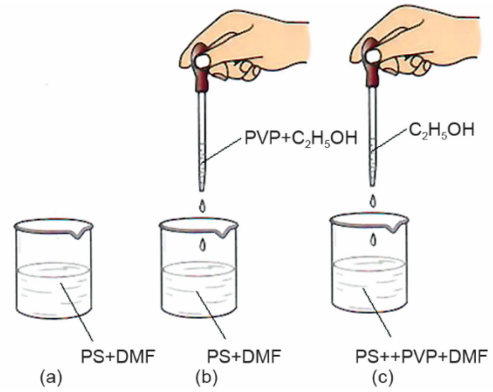

Figure 1. Spun solutions with different fractions of components and solvents

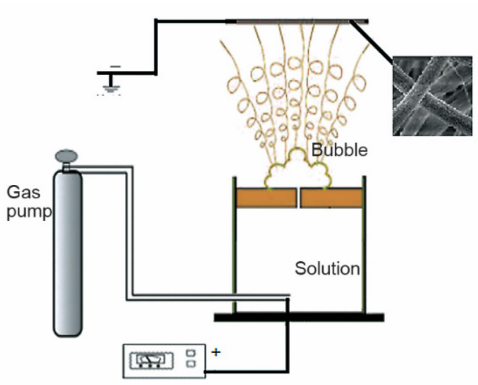

Figure 2. The bubble electrospinning

makes each debris lose solvents for a fast solidification. This evaporation process is similar to that in flash evaporation [9], and sometimes the solvents can be boiled due to the sudden pressure release, making a fast solvent evaporation. Additionally, due to high ejecting velocity of each debris, which is as high as 300 m/s, the air drag pushes the debris to form a fiber, and the surface tension makes the fiber cylindrical. According to Bernoulli equation:

$$\frac{1}{2}u^2 + \frac{P}{\rho} = B \tag{1}$$

where u is the velocity of the moving jet, P – the fluid pressure, ρ – the density, B – the Bernoulli constant. A debris from the broken bubble is accelerated from almost zero velocity to as high as 300 m/s, according to eq. (1), a great pressure drop occurs when the debris is ejected, this results in a second solvent evaporation in the spinning process. A spun solution with multiple fractions including solvents always leads to an extremely fast solvent evaporation, resulting in unsmooth surface of the obtained fibers.

Discussion and conclusion

Figure 3 is scanning electron microscope (SEM) of nanofibers from the sample A, and nanoscale pores are observed on fibers surface. Figure 4 is SEM of nanofibers from the sample D (PVP + C_2H_5OH). Figure 5 is SEM of nanofiber about liquid F.

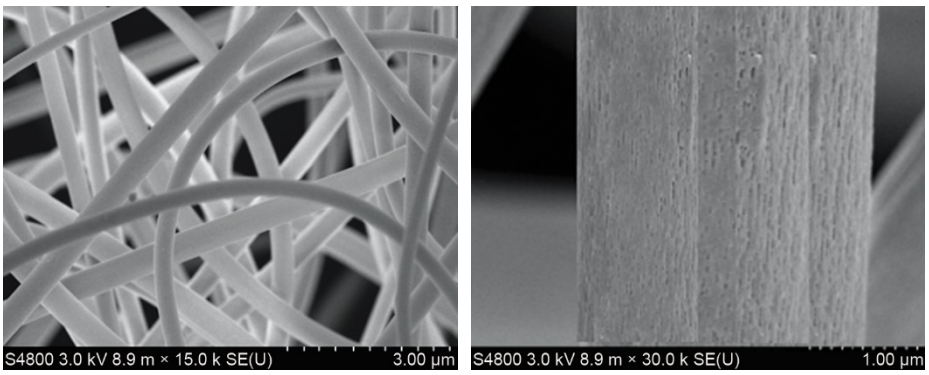

Figure 3. Nanofiber of PS

Figure 3(b) showed that the surface of PS nanofiber was porous nanostructure and rough, but fig. 4(b) displayed that the holes on the surface of PS/PVP composite nanofiber reduced obviously, and the rough degree of the surface was lowered clearly, while the smooth performance was improved. Although the components of nanofiber about fig. 5(b) were the same to that about fig. 4(b), there is a clear hierarchy structure on the surface of PS/PVP composite nanofiber. From fig. 5(b) we can see that the roughness of nanofiber surface is higher, there are more holes on the nanofiber surface, and even there are deep troughs on the nanofiber surface.

The components of nanofibers on figs. 4 and 5 are the same, but there are big differences about the surface morphology, this showed that the order ratio of solute and solvent in the solution have an effect on the hierarchy structure about the nanofiber surface [9, 10]. In fig. 4 we prepare the spinning solution on PS and PVP respectively, so even if when they are mixed their own dissolution was not destroyed, also good for bubble electrospinning, PVP can fill up the holes on the surface of PS nanofibers, so the holes on the surface of PVP nanofibers were reduced and it improve the smoothing effect of the surface. In fig. 5 we first let PVP and PS dissolve in DMF together. Because the ethanol and DMF are immiscible, so when the ethanol dropped into the aforementioned solution it had a greater influence on composite solution, which makes the surface of nanofiber appear unsmooth structure during the spinning process.

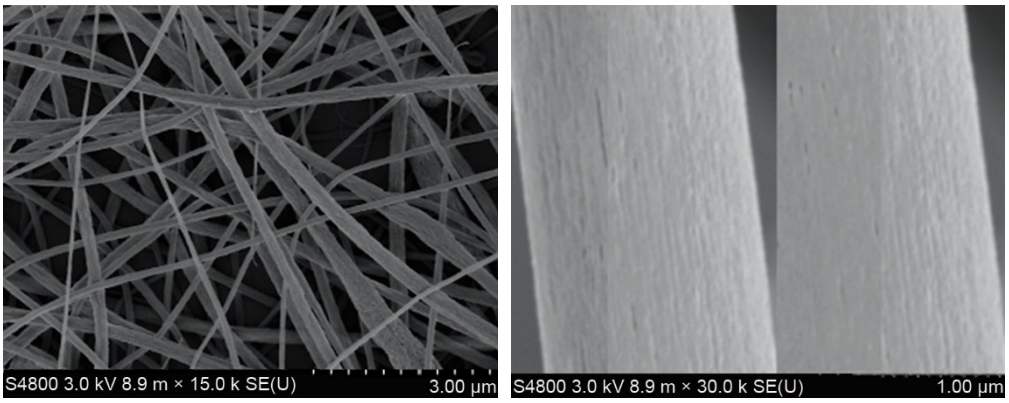

Figure 4. Composite nanofiber of PS/PVP(PS/DMF+PVP/C_2H_5OH)

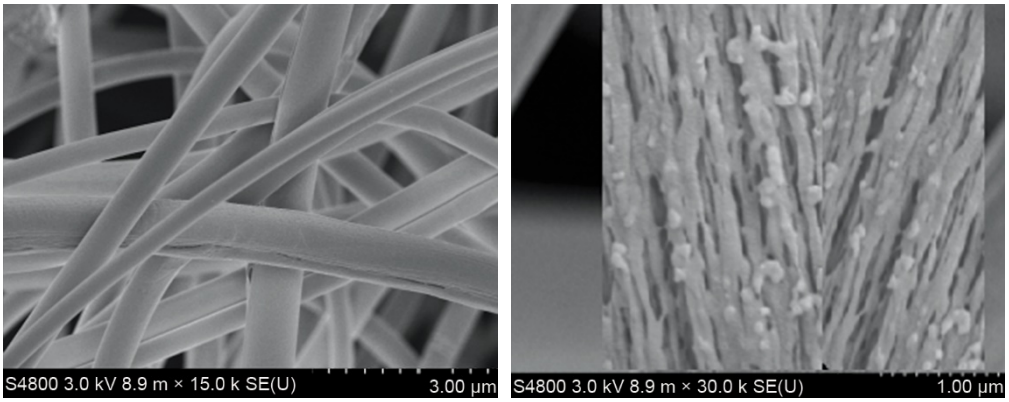

Figure 5. Composite nanofiber of PS/PVP(PS/PVP/DMF+C_2H_5OH)

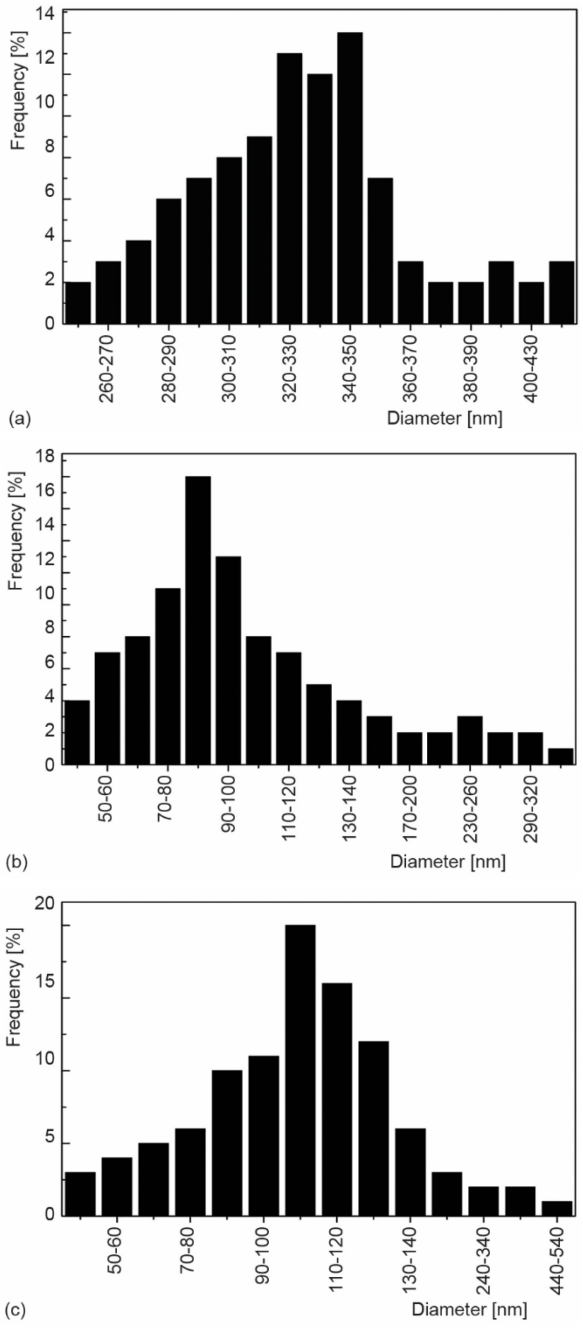

Figure 6. Diameter distribution of nanofiber in figs. 3-5

The diameter distribution of nanofibers in figs. 3-5, were shown in figs. 6(a)-(c), respectively. From fig. 6(a) we can find that the diameter of PS nanofibers range widely from 260 nm to 460 nm and its diameter concentrate between 310 nm and 360 nm. It can be seen from fig. 6(b) that during the same spinning technique, the diameter of PS/PVP composite nanofibers range narrowly from 40 nm to 350 nm, the diameter of most nanofibers concentrate between 50 nm to 130 nm. Although the fiber content of fig. 6(c) is same with that of fig. 6(b), due to the different preparation of spinning solution, we can find that the diameter of nanofibers about fig. 6(c) has changed from 40 nm to 540 nm, the diameter of nanofibers concentrate between 90 nm and 230 nm.

To discuss the effect of nanofiber surface unsmooth structure on hydrophilic performance, we test three water contact angles of the surface about those three kinds of nanofiber membranes. Water contact angle of nanomembrane shown in figs. 3-5 was shown in fig. 7. From fig. 7 we can see that in fig. 3 the PS nanofiber membrane surface water contact angle is 98°, in fig. 4 the PS/PVP composite nanofiber membrane surface contact angle is 108°, and in fig. 5 in the the PS/PVP composite nanofiber membrane surface contact angle is 83°, this hydrophilic differences is because of the nanofiber surface structure, the nanofiber surface in fig. 5 there has been a lot of grooves which make the fiber surface occurs capillary effect and improve the hydrophilicity of the nanofiber membranes.

In order to discuss the effect of fiber surface structure which was prepared by the new bubble electrospinning technology and spinning process on the nanomembrane tensile property, we respectively tested the tensile strength and tensile elongation rate of the aforementioned three nanomembranes, as shown in fig. 8. From fig. 8 we can see that alt-

hough the fiber components of the nanomembranes b and c were the same, nanomembrane c has the higher tensile strength and the smaller tensile elongation rate. This is because the high rough degree on the nanomembrane c surface increases fiber slip resistance [11].

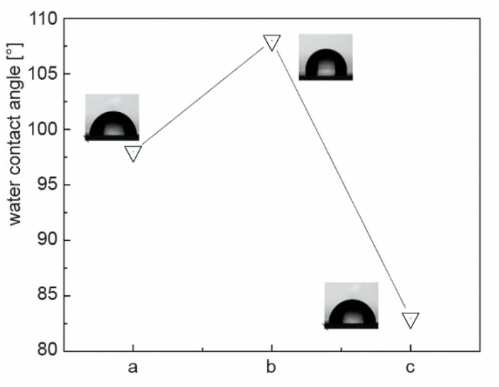

Figure 7. Water contact angle of nanomembrane in figs. 3-5

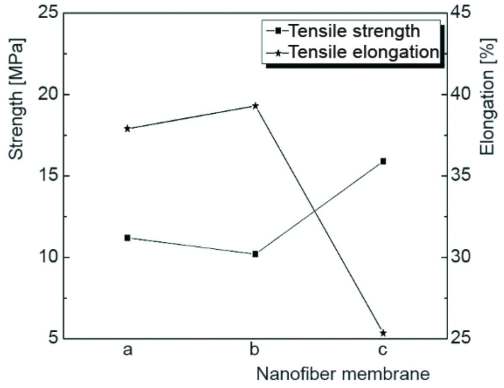

Figure 8. Tensile property of nanomembrane in figs. 3-5

The surface average pore size and air velocity of nanomembrane a, b, and c are shown in fig. 9. It can be seen in fig. 9 that the variation trend of the surface mean pore size keep consistent with that of the air velocity, and the nanomembrane c has the maximum surface average pore size and air velocity. Its main reasons were the unsmooth property on the surface and the more rough fiber diameter greatly increased opportunities of producing gap on the nanomembrane surface [12].

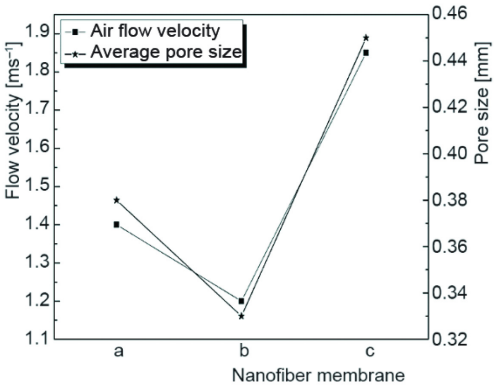

Figure 9. Average pore size and air-flow velocity of nanomembrane in figs. 3-5

Acknowledgment

The work is supported by Program for Industry University Research of Jiangsu Province under grant No. SBY2014020625, Key College Program of Yancheng Institute of Industry Technology under grant No. ygy1402, Introduction College Program of Yancheng Institute of Industry Technology under grant No. 2013-3800015. The work is also supported by Top-notch Academic Programs Project of Jiangsu Higher Education Institutions (PPZY2015C254), 2014 research Program of modern educational technology in Jiangsu Province (2014-R-31205), and 2015 National Natural Science Fund for youth (51503137).

References

[1] Wanjale, S., *et al.*, Surface Tailored PS/TiO_2 Composite Nanofiber Membrane for Copper Removal from Water, *Journal of Colloid and Interface Science, 469* (2016), 1 , pp. 31-37

[2] Ke, H. Z., *et al.*, Electrospun Polystyrene Nanofibrous Membranes for Direct Contact Membrane Distillation, *Journal of Membrane Science, 515* (2016), Oct., pp. 86-97
[3] Liu, X. H., *et al.*, Ultrasound-Mediated Preparation and Evaluation of a Collagen/PVP- PCL Micro- and Nanofiber Scaffold Electrospun from Chloroform/Ethanol Mixture, *Fibers and Polymers, 17* (2016), 8, pp. 1186-1197
[4] Jabbarnia, A., *et al.*, Investigating the Thermal, Mechanical, and Electrochemical Properties of PVDF/PVP Nanofibrous Membranes for Supercapacitor Applications, *Journal of Applied Polymer Science, 43037* (2016), Apr., pp. 1-10
[5] Afzali, M., *et al.*, Electrospun Composite Nanofibers of PolyVinyl Pyrrolidone and Zinc Oxide Nanoparticles Modified Carbon Paste Electrode for Electrochemical Detection of Curcumin, *Materials Science and Engineering, 68* (2016), Nov., pp. 789-797
[6] He, J.-H., *et al.*, Review on Fiber Morphology Obtained by Bubble Electrospinning and Blown Bubble Spinning, *Thermal Science, 16* (2012), 5, pp. 1263-1279
[7] He, J.-H., *et al.*, Control of Bubble Size and Bubble Number in Bubble Electrospinning, *Computers and Mathematics with Applications, 64* (2012), 18, pp. 1033-1035
[8] Zhao, L., *et al.*, Microstructure and Property of Regenepercentaged Silk Fibron/Chitosan Nanofibers, *Thermal Science, 20* (2016), 3, pp. 979-983
[9] Dou, H., *et al.*, A Belt-Like Super Fine Film Fabrication by the Bubble-Electrospinning, *Thermal Science, 17* (2013), 5, pp. 1508-1510
[10] Cheng, Y. L., *et al.*, Formation Mechanism of Fe_2O_3 Hollow Fibersby Direct Annealing of the Electrospun Composite Fibers and their Magnetic, Electrochemical Properties, *Cryst. Eng. Comm., 13* (2011), 8, pp. 2863-2870
[11] Wang, Z. Y., *et al.*, Preparation and Catalytic Property of PVDF Composite Membrane with Polymeric Spheres Decorated by Pd Nanoparticles in Membrane Pores, *Journal of Membrane Science*, *496* (2015), Dec., pp. 95-107
[12] Shin, Y. M., *et al.*, Electrospinning: A Whipping Fluid Jet Generates Submicron Polymer Fibers, *Applied Physics Letter*, *78* (2001), 8, p. 1149

Paper submitted: July 25, 2016
Paper revised: August 12, 2016
Paper accepted: September 20, 2016